Arab J Sci Eng (2012) 37:481–488
DOI 10.1007/s13369-012-0181-x

RESEARCH ARTICLE - CIVIL ENGINEERING

Franz-Josef Ulm

Nano-Engineering of Concrete

Received: 7 May 2010 / Accepted: 7 November 2010 / Published online: 31 January 2012

Abstract This paper summarizes recent developments in the field of nanoindentation analysis of highly heterogeneous composites. The fundamental idea of the proposed approach is that it is possible to assess nanostructure from the implementation of micromechanics-based scaling relations for a large array of nanoindentation tests on heterogeneous materials. We illustrate this approach through the application to calcium-silicate-hydrate (C-S-H), the binding phase of all cement-based materials. For this important class of materials, we show that C-S-H exists in at least three structurally distinct but compositionally similar forms: low density, high density and ultra-high density. These three forms differ merely in the packing density of 5-nm sized particles. The proposed approach also gives access to the solid particle properties of C-S-H, which can now be compared with results from atomistic simulations. By way of conclusion, we show how this approach provides a new way of analyzing complex hydrated nanocomposites, in addition to classical microscopy techniques and chemical analysis. This approach will turn out invaluable in our quest of adding the necessary "green" value to a commodity, concrete, by nano-engineering higher strength and toughness from first principles.

Keywords Calcium-silicate-hydrate · Concrete · Nano-engineering · Nanoindentation

الخلاصة

تلخص هذه الورقة التطورات الأخيرة في مجال تحليل nanoindentation للمواد غير المتجانسة إلى حد كبير. والفكرة الأساسية لهذا النهج المقترح هو أنه من الممكن تقييم البنية النانوية من تطبيق علاقات التحجيم المعتمدة على المايكروميكانيكا لمصفوفة كبيرة من اختبارات nanoindentation على مواد غير متجانسة. ولتوضيح هذا النهج خلال تطبيقة على هيدرات الكالسيوم سيليكات (C-S-H) الوجه الرابط لجميع المواد المعتمدة على الإسمنت. ولهذه الفئة المهمة من المواد فقد أوضحنا أن الـ(C-S-H) يتواجد في مالايقل عن ثلاثة أشكال إنشائية ولكنها متشابهة من حيث التكوين: الكثافة المنخفضة (LD) الكثافة العالية (HD) والفائقة الكثافة (UHD). هذه الاشكال الثلاثة تختلف فقط في كثافة التعبئة لحجم جسيمات خمسة نانومتر. إن النهج المقترح ايضا يعطي مدخلا لخواص الجزيئات الصلبة لـ C-S-H التي تقارن بالنتائج من المحاكاة الذرية. وعن طريق الاستنتاج فقد أوضحنا كيف أن هذا النهج يوفر طريقة جديدة لتحليل nanoindentation المعقدة. بالإضافة إلى تقنيات الفحص المجهري التقليدي والتحليل الكيميائي. وهذا النهج سوف يبين القيمة العالية في سعينا لإضافة القيمة الخضراء الضرورية للخرسانة بوساطة هندسة النانو العالية القوة والمتانة من المبادئ الأولى.

F.-J. Ulm (✉)
Massachusetts Institute of Technology,
Cambridge, MA, USA
E-mail: ulm@MIT.EDU

1 Introduction

More concrete is produced than any other synthetic material on Earth. The current worldwide cement production stands at 2.3 billion tons, enough to produce more than 20 billion tons or 1 cubic meter of concrete per capita per year. There is no other material that can replace concrete in the foreseeable future to meet our societies' legitimate needs for housing, shelter, infrastructure, and so on. But concrete faces an uncertain future, due to a non-negligible ecological footprint that amounts to 5–10% of the worldwide CO_2 production. It now appears that mechanics can be the discipline that enables the development of a sustainable green concrete future.

We here adopt the perspective originating from Galileo's Strength of Materials Theory, that weight, and thus CO_2-emission, increases with the volume of the produced material, while strength of structural members increases with the section. Hence, as one increases the strength of a material by a factor of λ, one reduces the environmental footprint by λ^{-1} for pure compressive members such as columns and perfect arches and shells, $\lambda^{-2/3}$ for beams in bending, and $\lambda^{-1/2}$ for slabs. Similarly, if one adopted a linear elastic fracture model, an increase of the fracture toughness $K_{\mathrm{Ic}} = \mu K^0_{\mathrm{Ic}}$, would entail a reduction of the environmental footprint by μ^{-1} for columns and $\mu^{-4/5}$ for (notched) beams in bending or in torsion. Arguably, since these gains in reducing the environmental footprint, lead to slender concrete structures, they are limited for compressive members by buckling and for bending members by deflection, for which in both cases $\lambda^{-1/4}$ (when assuming a square-root relation between Young's modulus and strength according to currents standards; e.g. [1]). All this hints towards a critical role of mechanics, and in particular Strength of Materials and Fracture Mechanics, in redesigning concrete materials and structures for the coming of age of global warming. In contrast to the classical top-down empirical approaches, we have chosen a bottom-up approach that starts at the electron and atomic scale to nanoengineer the fundamental building block of concrete; to assess the properties by nanoindentation; and upscale strength, fracture and stiffness properties from nanoscales to macroscales of day-to-day concrete engineering applications. The key to all this is mechanics at the interface of physics and engineering.

With this in mind, this paper summarizes recent developments in the field of nanoindentation analysis of highly heterogeneous composites. One of the most promising techniques that emerged from the implementation of nanotechnology in material science and engineering to assess mechanical properties at small scales is nanoindentation. The idea is simple: by pushing a needle onto the surface of a material, the surface deforms in a way that reflects the mechanical properties of the indented material. Yet, in contrast to most metals and ceramics, for which this technique was originally developed, most materials relevant to civil engineering, petroleum engineering or geophysical applications are highly heterogeneous from a scale of a few nanometers to macroscopic scales. The most prominent heterogeneity is the porosity.

Take, for instance, the case of concrete. Groundbreaking contributions date back to the 1950s with the work of Powers and his colleagues [22], who by correlating macroscopic strength [13] and stiffness data [38] with physical data of a large range of materials prepared at different *w*/*c*-ratios early on recognized the critical role of the C-S-H porosity (or gel porosity), respectively, the C-S-H packing ("one minus porosity") on the macroscopic mechanical behavior; in particular for cement pastes with water-to-cement ratios (*w*/*c*) below 0.42, for which the entire porosity of the material is situated within the C-S-H (no "capillary water" in powers' terminology), and for which the hydration degree α of the hardened material is smaller than one. Powers considered the C-S-H gel porosity (gel pore volume over total gel volume) to be material invariant and equal to $\phi_0 = 0.28$ independent of mix proportions, hydration degree, C-S-H morphology, etc. The application of advanced microscopy, X-ray mapping and Neutron scattering techniques to cement-based materials later on revealed that the assumption of a constant gel porosity could not be but an oversimplification of the highly heterogeneous nanostructure of cement-based materials, overlooking the particular organizational feature of cement hydration products in highly dense packed "inner" products and loosely packed "outer" products; see, for instance [7,12,23–25,27,29–31,33,39]. The quantitative translation of these morphological observations into a concise microstructure model of the gel microstructure is due to Jennings and co-worker [15–18,32], who recognized that outer and inner products are two structurally distinct but compositionally similar C-S-H phases; that is, amorphous nanoparticles of some 5-nm characteristic size pack into two characteristic forms, a low density (LD) C-S-H phase and a high density (HD) C-S-H phase, that can be associated with outer and inner products. The existence and mechanical importance of these phases have been confirmed by nanoindentation [4,6,35]: LD C-S-H and HD C-S-H were found to be uniquely characterized by a set of material properties that do no depend on mix proportions, type of cement, etc. Instead, they are intrinsic material invariant properties. The link between these mechanical C-S-H phase properties and C-S-H packing density has been established, showing that the C-S-H phases exhibit a unique nanogranular morphology [5,8,18], with packing densities that

come remarkably close to limit packing densities of spheres; namely the random close-packed limit (RCP) [14] or maximally random jammed state (MRJ) [9] of $\eta = 0.64$ for the LD C-S-H phase; and the ordered face-centered cubic (fcc) or hexagonal close-packed (hcp) packing of $\eta = \pi/\sqrt{18} = 0.74$ [28] for the HD C-S-H phase. Far from being constant, the gel porosity of the C-S-H phase is recognized, in this model, to depend on the volume proportions of LD C-S-H (f_{LD}) and HD C-S-H (f_{HD}) [35]:

$$\phi_0 = 1 - (0.64 \times f_{\mathrm{LD}} + 0.74 \times f_{\mathrm{HD}}) \tag{1}$$

The focus of this paper is to review some recent developments in the field of nanoindentation analysis of highly heterogeneous materials. Illustrated through the example of concrete, the approach proposed here can equally be applied to many other highly heterogeneous materials whose material behavior is governed by porosity (bones, shale etc. [2,36]).

2 Micromechanics-Based Nanoindentation Techniques

Consider an indentation test in a porous material, the characteristic size of the porosity being such that scale separability applies. The indenter is at a depth h, and what is sensed in the indentation test is a composite response of the solid phase and the porosity. That is, the hardness H and the indentation modulus M determined from the load–depth (P–h) curve according to classical indentation analysis tools [20] are representative of the particle properties [particle stiffness m_{s}, hardness h_{s}, (Drucker-Prager) friction coefficient μ], and of the packing of their particles (packing density η), and some morphological parameters (denoted by η_0) [36]:

$$\begin{aligned} H &= \frac{P}{A_{\mathrm{c}}} = h_{\mathrm{s}} \times \Pi_H(\mu, \eta, \eta_0) \\ M &= c\frac{(\mathrm{d}P/\mathrm{d}h)_{h_{\max}}}{\sqrt{A_{\mathrm{c}}}} = m_{\mathrm{s}} \times \Pi_M(\nu, \eta, \eta_0) \end{aligned} \tag{2}$$

where A_{c} is the projected contact area, and Π_H and Π_M are dimensionless functions and ν = Poisson's ratio. Linear and nonlinear microporomechanics [10] provides a convenient way to determine these functions.

2.1 Does Particle Shape Matter? [34]

The determination of functions Π_H and Π_M requires the choice of particle morphology. For perfectly disordered materials, the key quantity to be considered is the percolation threshold, that is the critical packing density below which the composite material has no strength nor stiffness. This percolation threshold depends on the particle shape [26]. Clearly, as seen in TEM images of C-S-H, the elementary particle has an aspect ratio. However, as far as the mechanics response is concerned, it turns out that particle shape does not matter as soon as the packing density of the porous material is greater than 60%. This is obviously the case of cement-based materials (as their industrial success is due to their strength performance), and also of most other natural composite materials like bone, compacted clays (shale), etc. One can thus conclude that the effect of particle shape is negligible as far as the mechanical performance is concerned [34]; see Fig. 1.

2.2 Micromechanics-Based Scaling Functions [3,11]

The negligible effect of the particle shape on the homogenized mechanical properties largely simplifies the micromechanical analysis. It thus suffices, to consider spherical particles and a distinct disordered morphology of the solid phase, similar to a polycrystal, characterized by a solid percolation threshold of $\eta_0 = 0.5$. Based on linear micromechanics of the indentation modulus, a good approximation (which is exact for a solid Poisson's ratio of $\nu = 0.2$) is a linear scaling [5]:

$$\frac{M}{m_{\mathrm{s}}} = \Pi_M = \langle 2\eta - 1 \rangle \tag{3}$$

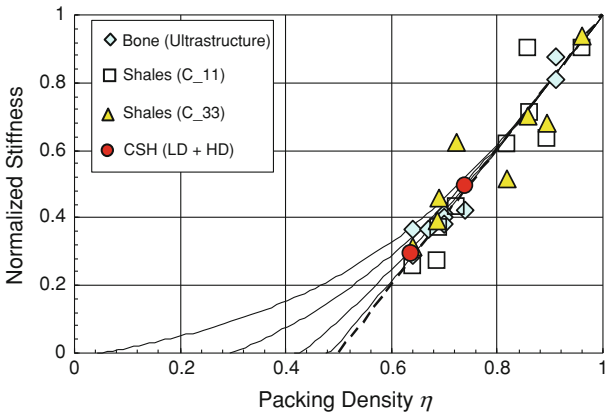

Fig. 1 Normalized stiffness versus packing density scaling relations. The percolation threshold of 0.5 corresponds to a perfectly disordered material composed of spherical particles, while lower percolation thresholds are representative of disordered materials with particle shape (here ellipsoids). Adapted from [34]

Using a similar approach for strength homogenization, an appropriate scaling for hardness is [3,11]:

$$\frac{H}{h_s} = \Pi_H = \Pi_1(\eta) + \mu(1-\eta)\Pi_2(\mu,\eta) \tag{4}$$

where:

$$\Pi_1(\eta) = \frac{\sqrt{2(2\eta-1)} - (2\eta-1)}{\sqrt{2}-1}(1 + a(1-\eta) + b(1-\eta)^2 + c(1-\eta)^3)$$
$$\Pi_2(\mu,\eta) = \frac{2\eta-1}{2}(d + e(1-\eta) + f(1-\eta)\mu + g\mu^3) \tag{5}$$

and where $a = -5.3678$, $b = 12.1933$, $c = -10.3071$, $d = 6.7374$, $e = -39.5893$, $f = 34.3216$ and $g = -21.2053$ are all constants associated with a Berkovich indenter geometry and a polycrystal morphology with percolation threshold of $\eta_0 = 0.5$.

2.3 Implementation for Back-Analysis of Packing Density [36]

Consider then a series of N indentation tests on a heterogeneous material. What is measured in these tests are N times (M, H) values at each indentation point representative of a composite response. Assuming that the solid phase is the same, and all what changes between indentation points are the packing density, there are three particle unknowns (m_s, h_s, μ) and N packing densities. Hence, for $N \gg 3$, the system is highly over determined, which makes it possible to assess microstructure and particle properties. A typical example of this implementation of micromechanics-based scaling relations to analyze packing density is shown in Fig. 2.

3 Packing Density Distributions of C-S-H

By way of application, we apply this method to analyze packing density distributions for different cement paste materials. In a first step, we deconvolute the packing density together with indentation modulus and indentation hardness to obtain mean values and standard deviations of different phases. This is shown in Fig. 3. This type of analysis is performed for a large range of cement pastes prepared with different *w/c* ratios. The results, which are shown in Fig. 4, call for the following comments:

- The packing density distributions (Fig. 3) for different *w/c* provide strong evidence of three statistically significant C-S-H phases; namely a ultra-high density (UHD) C-S-H phase, in addition to the already known LD C-S-H and HD C-S-H phases. The nanomechanical properties of the UHD C-S-H phase, M and H, are found to follow similar packing density scaling relations as LD C-S-H and HD C-S-H. This suggests that

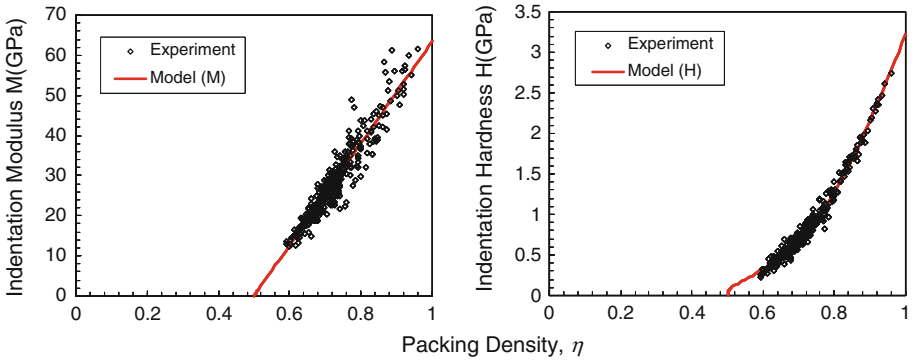

Fig. 2 Micromechanics-based scaling relations of the packing density of indentation modulus and indentation hardness for a $w/c = 0.4$ cement paste. Adapted from [36]

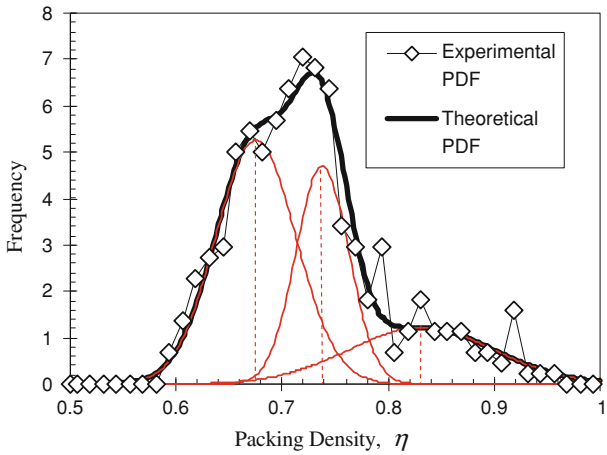

Fig. 3 Packing density distribution for a $w/c = 0.4$ cement paste. Adapted from [36]

the UHD C-S-H phase is structurally distinct but compositionally similar to the other C-S-H phases. That is, it is made of the same elementary building block, the C-S-H solid, and differs from LD and HD C-S-H only in its characteristic packing density. The UHD C-S-H phase has a packing density of $\eta = 0.83 \pm 7\%$, which comes remarkably close to a two-scale limit random packing of $0.64 + (1 - 0.64) \times 0.64 = 0.87$.

- An increase of the *w/c* ratio entails an increase in the hydration degree, α (Fig. 4a), estimated here as the volume amount of phases that exhibit an indentation modulus smaller than ~ 63 GPa. In turn, this increase is due an increase in similar proportions of both the C-S-H solid and the gel porosity; roughly 5% per 0.1 increase in *w/c*.
- The increase with the *w/c* ratio of both the C-S-H solid and the gel porosity in similar proportions has different effects on the microstructure organization of the hydration products into LD C-S-H, HD C-S-H and UHD C-S-H (Fig. 4b): Above $w/c = 0.2$, the volume occupied by UHD C-S-H—among the hydration products—is almost constant (20%), while the decrease in HD C-S-H is compensated by the formation of LD C-S-H: at low *w/c*, HD C-S-H dominates over LD C-S-H, while it is inverse at high *w/c* ratios.
- An extremely low $w/c = 0.15$, characterized by a hydration degree on the order of $\alpha = 0.6$, a 10% gel porosity and a 50% C-S-H solid volume fraction, favors almost exclusively the formation of the UHD C-S-H phase.

In summary, while the water available for hydration increases the amount of hydration solid, it appears that the concurrent increase in gel porosity favors the formation of looser packed LD C-S-H to the detriment of HD C-S-H; while the UHD C-S-H phase remains almost constant.

Finally, it is interesting to locate these different phases in the microstructure. This can be achieved by spatially mapping the indentation results on a grid. To this end, we performed a series of 900 nanoindentations on a tightly spaced grid, with a spacing of 3 μm between nanoindents. After deconvolution of the 900 nanoindentations, and application of the micromechanics-based scaling relations, to each phase (LD C-S-H, HD

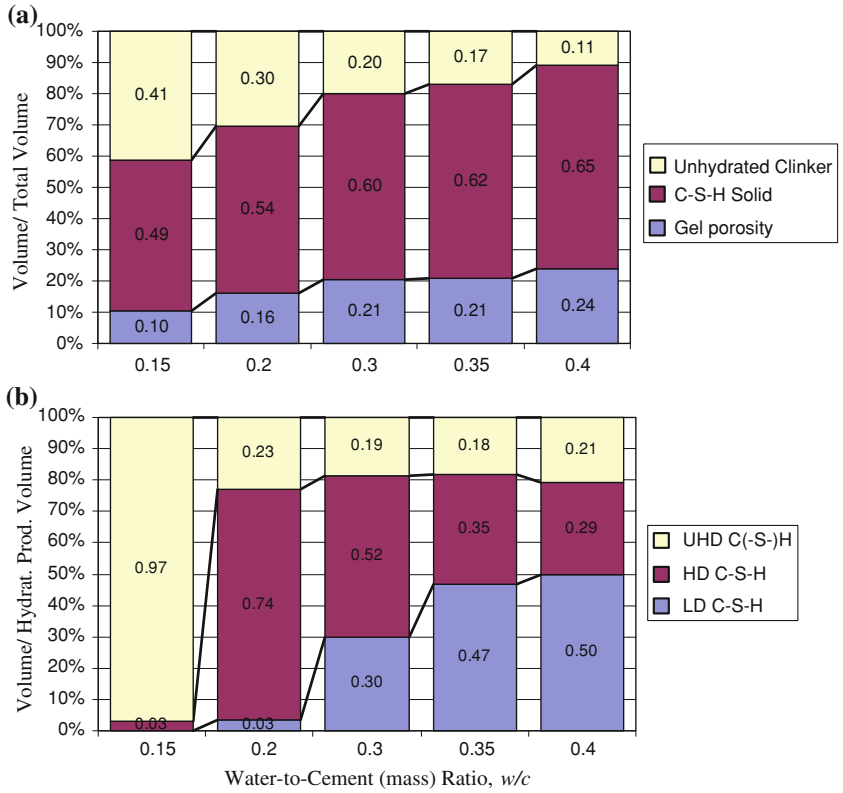

Fig. 4 Volume fraction distributions in the microstructure: **a** volume fractions of the cement paste composite; **b** volume fractions of the hydration phases. Adapted from [37]

C-S-H, UHD C-S-H and clinker) is associated as an interval of packing density. By doing so, each specific point on the grid of nanoindentations can be associated with the phase on which the nanoindentation was performed. Such a technique provides a mechanical mapping of the indented surface with an accuracy limited by the grid spacing. The results of this mapping are displayed in Fig. 5a for a $w/c = 0.2$ material and in Fig. 5b for a $w/c = 0.3$ material.

Similar to HD C-S-H, UHD C-S-H can primarily (i.e. in significant amount) be found close to the clinker grains. A similar observation of a high stiffness phase in the vicinity of clinker grain was also reported in [19]. Some areas of UHD C-S-H are also visible far from clinker grains. Yet, this occurrence may be attributed to the presence of a clinker grain below the surface; a conjecture that cannot be resolved with the surface mapping technique employed here. In return, a comparison of the amount of the different C-S-H phases present in the two materials clearly shows that HD C-S-H and UHD C-S-H dominate low *w/c* materials, while higher *w/c* materials are increasingly dominated by LD C-S-H.

4 Concluding Remarks

Nanoindentation has originally been developed to assess mechanical properties at very fine scales; but its application to highly heterogeneous materials has provided the materials science community with a wealth of new information about morphology of elementary particles; thanks to the application of micromechanics-based indentation analysis tools that link mechanical properties to microstructure and constituent properties.

It is of great interest to compare the particle properties so obtained with particle properties of C-S-H obtained by atomistic simulations. Such atomistic simulations of a realistic C-S-H model provide a particle stiffness of $m_s = 65$ GPa using the elasticity constants, the Reuss-Voigt-Hill average, and a maximum negative isotropic pressure before rupture of the simulation cell perpendicular to the layer plane of $h_s = 3$ GPa [21]. These values are in very good agreement with the asymptotic values obtained from the micromechanics-based scaling relations (Fig. 2). Hence, a combination of nanoindentation, micromechanics-based scaling

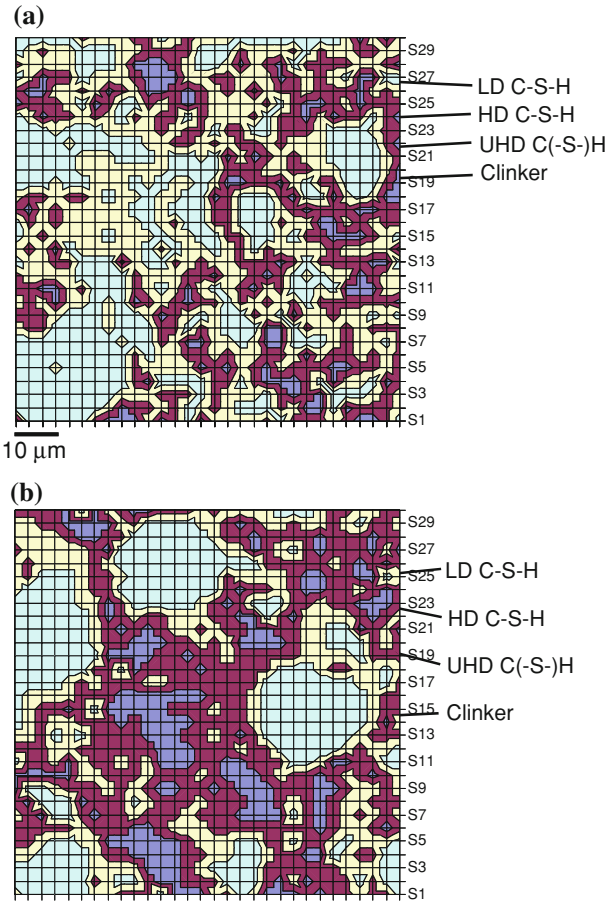

Fig. 5 Mechanical mapping of LD C-S-H, HD C-S-H, UHD C(-S-)H and clinker phases in **a** a $w/c = 0.2$ hardened cement paste; **b** a $w/c = 0.3$ hardened cement paste. Adapted from [37]

relations and atomistic simulations provides a means to bridge between the atomistic structure of C-S-H, its nanomechanical morphology and macroscopic performance.

We are thus one step closer to implementing the Materials Science Paradigm for highly heterogeneous materials like concrete, bones, shale etc., linking composition with microstructure, and to ultimately predicting ("nanoengineering") macroscopic mechanical performance of this class of hydrated nanocomposites based on composition and microstructure. This will turn out invaluable in our quest of adding the necessary "green" value to a commodity: concrete.

Acknowledgments Revised and expanded version of a review paper presented at NICOM-3, Prague, on June 2, 2009. Material and financial support of this research through Lafarge Corporation is gratefully acknowledged.

References

1. ACI Committee 318: Building code requirements for reinforced concrete (ACI 318-95). American Concrete Institute, Farmington Hills (1995)
2. Bobko, C.; Ulm, F.-J.: The nano-mechanical morphology of shale. Mech. Mater. **40**(4–5), 318–337 (2008)
3. Cariou, S.; Ulm, F.J.; Dormieux, L.: Hardness-packing density scaling relations for cohesive-frictional porous materials. J. Mech. Phys. Solids. **56**, 924–952 (2008)
4. Constantinides, G.; Ulm, F.-J.: The effect of two types of C-S-H on the elasticity of cement-based materials: results from nanoindentation and micromechanical modeling. Cem. Concr. Res. **34**(1), 67–80 (2004)
5. Constantinides, G.; Ulm, F.-J.: The nanogranular nature of C-S-H. J. Mech. Phys. Solids. **55**(1), 64–90 (2007)
6. Constantinides, G.; Ulm, F.-J.; Van Vliet, K.: On the use of nanoindentation for cementitious materials. Mater. Struct. **36**(3), 191–196 (2003)
7. Dalgleish, B.J.; Ibe, K.: "Thin foil studies of hydrated cements." Cement and Concrete Research. **11**, 729–739 (1981)

8. DeJong, M.J.; Ulm, F.-J.: The nanogranular behavior of C-S-H at elevated temperatures (up to 700°C). Cem. Concr. Res. **37**(1), 1–12 (2007)
9. Donev, A.; Cisse, I.; Sachs, D.; Variano, E.A.; Stillinger, F.H.; Connely, R.; Torquato, S.; Chaikin, P.M.: Improving the density of jammed disordered packings using ellipsoids. Science. **303**, 990–993 (2004)
10. Dormieux, L.; Kondo, D.; Ulm, F.-J.: Microporomechanics. Wiley, UK (2006)
11. Gathier, B.; Ulm, F.-J.: Multiscale strength homogenization - application to shale nanoindentation. MIT-CEE Res. Rep. R08-01, Dept. of Civil and Environmental Engineering, Massachusetts Institute of Technology, Cambridge (2008)
12. Groves, G.W.: TEM studies of cement hydration. Mat. Res. Soc. Symposium Proc. **85**, 3–12 (1987)
13. Helmuth, R.A.; Turk, D.H.: Elastic moduli of hardened portland cement and tricalcium silicate pastes: effect of porosity. In: Symposium on structure of Portland cement paste and concrete, pp. 135–144 (1966)
14. Jaeger, H.M.; Nagel, S.R.: Physics of granular state. Science. **255**(5051), 1523–1531 (1992)
15. Jennings, H.M.: A model for the microstructure of calcium silicate hydrate in cement paste. Cem. Concr. Res. **30**, 101–116 (2000)
16. Jennings, H.M.: Colloid model of C-S-H and implications to the problem of creep and shrinkage. Mat. Struct. **37** (265), 59–70 (2004)
17. Jennings, H.M.: Refinements to colloid model of C-S-H in cement: CM-II. Cem Concr Res. **38** (3), 275–289 (2008)
18. Jennings, H.M.; Thomas, J.J.; Gevrenov, J.S.; Constantinides, G.; Ulm, F-J.: A multi-technique investigation of the nanoporosity of cement paste. Cem. Concr. Res. **37** (3), 329–336 (2007)
19. Mondal, P.; Shah, S.P.; Marks, L.: A reliable technique to determine the local mechanical properties at the nanoscale for cementitious materials. Cem. Concr. Res. **37**(10), 1440–1444 (2007)
20. Oliver, W.C.; Pharr, G.M.: An improved technique for determining hardness and elastic modulus using load and displacement sensing indentation experiments. J. Mater. Res. **7**(6), 1564–1583 (1992)
21. Pellenq, R.J.M.; et al.: A realistic molecular model of cement hydrates. PNAS. **106**(38), 16102–16107 (2009)
22. Powers, T.C.; Brownyard, T.L.: Studies of the physical properties of hardened Portland cement paste. Bull. 22, Res. Lab. of Portland Cement Association, Skokie, IL, U.S. J. Am. Concr. Inst. (Proc.), 43 (1947) 101–132, 249–336, 469–505, 549–602, 669–712, 845–880, 933–992 (reprint) (1947)
23. Richardson, I.G.: The nature of C-S-H in hardened cements. Cem. Concr. Res. **29**, 1131–1147 (1999)
24. Richardson, I.G.: "Tobermorite/jennite- and tobermorite/calcium hydroxide-based models for the structure of C-S-H: applicability to hardened pastes of tricalcium silicate, β-dicalcium silicate, Portland cement, and blends of Portland cement with blast-furnace slag, metakaolin, or silica fume. Cem. Concr. Res. **34**, 1733–1777 (2004)
25. Richardson, I.G.; Rodger, S.A.; Groves, G.W.: The porosity and pore structure of hydrated cement pastes as revealed by electron microscopy techniques. Mat. Res. Soc. Symp. Proc. **137**, 313–318 (1989)
26. Sanahuja, J.; Dormieux, L.; Chanvillard, G.: Modelling elasticity of a hydrating cement paste. Cem. Concr. Res. **37**, 1427–1439 (2007)
27. Scrivener, K.L.; Patell, H.H.; Pratt, P.L.; Parrott, L.J.: Analysis of phases in cement paste using backscattered electron images, methanol adsorption and thermogravimetric analysis. Mat. Res. Soc. Symp. Proc. **85**, 67–76 (1985)
28. Sloane, N.J.A.: Kepler's conjecture confirmed. Nature. **395**, 435–436 (1998)
29. Taplin, J.H.: A method for following the hydration reaction in portland cement paste. Aust. J. Appl. Sci. **10**, 329–345 (1959)
30. Taylor, H.F.W.: Studies on the chemistry and microstructure of cement pastes. Proc. Brit. Ceram. Soc. **35**, 65–82 (1984a)
31. Taylor, H.F.W.: Newbury DE, An electron microprobe study of a mature cement paste. Cem. Concr. Res. **14**, 565–573 (1984b)
32. Tennis, P.D.; Jennings, H.M.: A model for two types of calcium silicate hydrate in the microstructure of portland cement pastes. Cem. Concr. Res. **30**, 855–863 (2000)
33. Thomas, J.J.; Jennings, H.M.; Allen, A.J.: The surface area of cement paste as measured by neutron scattering: evidence for two C-S-H morphologies. Cem. Concr. Res. **28**(6), 897–905
34. Ulm, F.J.; Jennings, H.M.: Does C-S-H particle shape matter? A discussion of the paper 'Modelling elasticity of a hydrating cement paste', by Julien Sanahuja, Luc Dormieux and Gilles Chanvillard. CCR 37 (2007) 1427–1439. Cem. Concr. Res. **38**(8–9), 1126–1129 (2008)
35. Ulm, F-J.; Constantinides, G.; Heukamp, F.H.: Is concrete a poromechanics material? A multiscale investigation of poroelastic properties. Mater. Struct. **37** (265), 43–58 (2004)
36. Ulm, F.J.; Vandamme, M.; Bobko, C.; Ortega, J.A.; Tai, K.; Ortiz, C.: Statistical indentation techniques for hydrated nanocomposites: concrete, bone, and shale. J. Am. Ceram. Soc. **90**(9), 2677–2692 (2007)
37. Vandamme, M.; Ulm, F-J.; Fonollosa, P.: Nanogranular packing of C-S-H at substochiometric conditions. Cem. Concr. Res. **40**, 14–26 (2010)
38. Verbeck, G.J.; Helmuth, R.A.: Structures and physical properties of cement paste. In: 5th Internaional congress cement chemistry, Tokyo, pp. 1–44 (1969)
39. Viehland, D.; Li, J.F.; Yuan, L.J.; Xu, Z.K.: Mesostructure of calcium silicate hydrate (C-S-H) gels in portland-cement paste-a short range ordering nanocrystallinity and local compositional order. J. Am. Ceram. Soc. **79**(7), 1731–1744 (1996)